European Journal of Radiology Open 12 (2024) 100548

Contents lists available at ScienceDirect

European Journal of Radiology Open

journal homepage: www.elsevier.com/locate/ejro

Multisequence MRI-based radiomics signature as potential biomarkers for differentiating KRAS mutations in non-small cell lung cancer with brain metastases

Xinna Lv [a], Ye Li [a], Bing Wang [b], Yichuan Wang [b], Zexuan Xu [a], Dailun Hou [a,*]

[a] Beijing Chest Hospital, Capital Medical University, Beijing 101149, China
[b] Beijing Tuberculosis and Thoracic Tumor Research Institute, Beijing 101149, China

ARTICLE INFO

Keywords:
Machine learning
Radiomics
Magnetic resonance imaging
Kirsten rat sarcoma virus
Brain metastases

ABSTRACT

Background: Kirsten rat sarcoma virus (KRAS) has evolved from a genotype with predictive value to a therapeutic target recently. The study aimed to establish non-invasive radiomics models based on MRI to discriminate KRAS from epidermal growth factor receptor (EGFR) or anaplastic lymphoma kinase (ALK) mutations in lung cancer patients with brain metastases (BM), then further explore the optimal sequence for prediction.

Methods: This retrospective study involved 317 patients (218 patients in training cohort and 99 patients in testing cohort) who had confirmed of KRAS, EGFR or ALK mutations. Radiomics features were separately extracted from T2WI, T2 fluid-attenuated inversion recovery (T2-FLAIR), diffusion weighted imaging (DWI) and contrast-enhanced T1-weighted imaging (T1-CE) sequences. The maximal information coefficient and recursive feature elimination method were used to select informative features. Then we built four radiomics models for differentiating KRAS from EGFR or ALK using random forest classifier. ROC curves were used to validate the capability of the models.

Results: The four radiomics models for discriminating KRAS from EGFR all worked well, especially DWI and T2WI models (AUCs: 0.942, 0.942 in training cohort, 0.949, 0.954 in testing cohort). When KRAS compared to ALK, DWI and T2-FLAIR models showed excellent performance in two cohorts (AUCs: 0.947, 0.917 in training cohort, 0.850, 0.824 in testing cohort).

Conclusions: Radiomics classifiers integrating MRI have potential to discriminate KRAS from EGFR or ALK, which are helpful to guide treatment and facilitate the discovery of new approaches capable of achieving this long-sought goal of cure in lung cancer patients with KRAS.

1. Introduction

Brain metastases (BM) are the most common intracranial tumor in adults with an extremely poor prognosis [1]. Lung cancer (LC) has the highest frequency to metastasize to the brain that accounts for 40–50% of BM cases [1]. Increasing evidence has demonstrated that the mutation status in the primary tumor was also present in the metastases [2]. Recently, targeted therapies have significantly prolonged progression-free survival for non-small cell lung cancer (NSCLC) patients with BM, particularly in patients with specific genetic mutations [3]. Currently, epidermal growth factor receptor (EGFR) mutations, anaplastic lymphoma kinase (ALK) rearrangements and Kirsten rat sarcoma virus (KRAS) are the most commonly tested oncogenic targets of NSCLC [4]. Moreover, multiple researches have shown that EGFR

Abbreviations: ALK, Anaplastic lymphoma kinase; AUC, Area under the ROC curve; BM, Brain metastases; CNS, Central nervous system; DWI, Diffusion weighted imaging; EGFR, Epidermal growth factor receptor; GLCM, Grey level co-occurrence matrix; GLRLM, Grey level run length matrix; GLSZM, Grey level size zone matrix; GLDM, Grey level dependence matrix; KRAS, Kirsten rat sarcoma virus; LC, Lung cancer; MIC, Maximal information coefficient; MRI, Magnetic resonance imaging; NGTDM, Neighbouring grey tone difference matrix; NSCLC, Non-small cell lung cancer; SMOTE, Synthetic minority oversampling technique; T1-CE, Contrast-enhanced T1-weighted imaging; T2-FLAIR, T2 fluid-attenuated inversion recovery; TI, Inversion time; RFC, Random forest classifier; RFE, recursive feature elimination; ROI, Region of interest; ROC, Receiver operator characteristic curve.

* Corresponding author.
E-mail address: hou.dl@mail.ccmu.edu.cn (D. Hou).

https://doi.org/10.1016/j.ejro.2024.100548
Received 9 October 2023; Received in revised form 8 January 2024; Accepted 11 January 2024
2352-0477/© 2024 The Authors. Published by Elsevier Ltd. This is an open access article under the CC BY-NC-ND license (http://creativecommons.org/licenses/by-nc-nd/4.0/).

mutations and ALK rearrangements are prone to developing BM, potentially associated with the extended survival for patients treated with systemic therapy [5,6]. However, unlike above two clinically actionable mutation status, KRAS which accounted for approximately 20–25% of NSCLC was once considered not targetable [7,8]. Recently, KRAS has lost its title as "undruggable" officially with the approval of the KRAS G12C inhibitor [9]. Whereas, the data on the KRAS G12C inhibitors have shown that these agents are far from curative and substantial clinical practice is ongoing to further advance KRAS-targeted therapy [9]. Therefore, timely differentiating KRAS from EGFR or ALK not only guides targeted treatment strategies but also gets patients harboring KRAS mutations to join the clinical investigation as early as possible which could drive the development of effective treatments.

Pathological examination through puncture biopsy is the gold standard for confirming genetic status. Nevertheless, because of its invasive nature, it is impractical and unrepeatable to obtain tissue samples from primary lesions or BM in some cases [10]. Magnetic resonance imaging (MRI) is the most significant tool to diagnose and monitor BM now [11]. Although MRI can clearly reflect the characteristics of BM, it still requires substantial work and show strong variation between readers [10], particularly cannot provide molecular and genetic information. Developing a non-invasive, reproducible and easy-to-use method that can evaluate the whole tumor to help identify mutation status of BM would assist histological assessment. Radiomics is an emerging field of research associated with the extraction of radiomics features within medical images [12]. These quantitative metrics can describe tumor genotype or molecular phenotype and provide more detailed information than would be possible by human eyes [10,12]. Hence, MR images reflecting the whole tumor volume can be deeply mined by radiomics.

Several studies have reported that a machine learning-derived radiomics approach based on CT image features in patients with NSCLC can predict the mutation status [13,14]. However, with the popularization and development of MRI, increasing number of small BM in asymptomatic patients can be detected even prior to the primary tumor [15]. There was limited literature to detect genetic mutation for LC patients with BM using MRI radiomics [16], especially the study related to identifying KRAS from the other two common mutation types. The aim of our study was to build and validate machine learning models based on MRI of BM to differentiate KRAS from EGFR or ALK mutations and explore the optimal MR sequence for predication.

2. Methods

2.1. Participants

This study was approved by the Ethics Committee of local hospital.

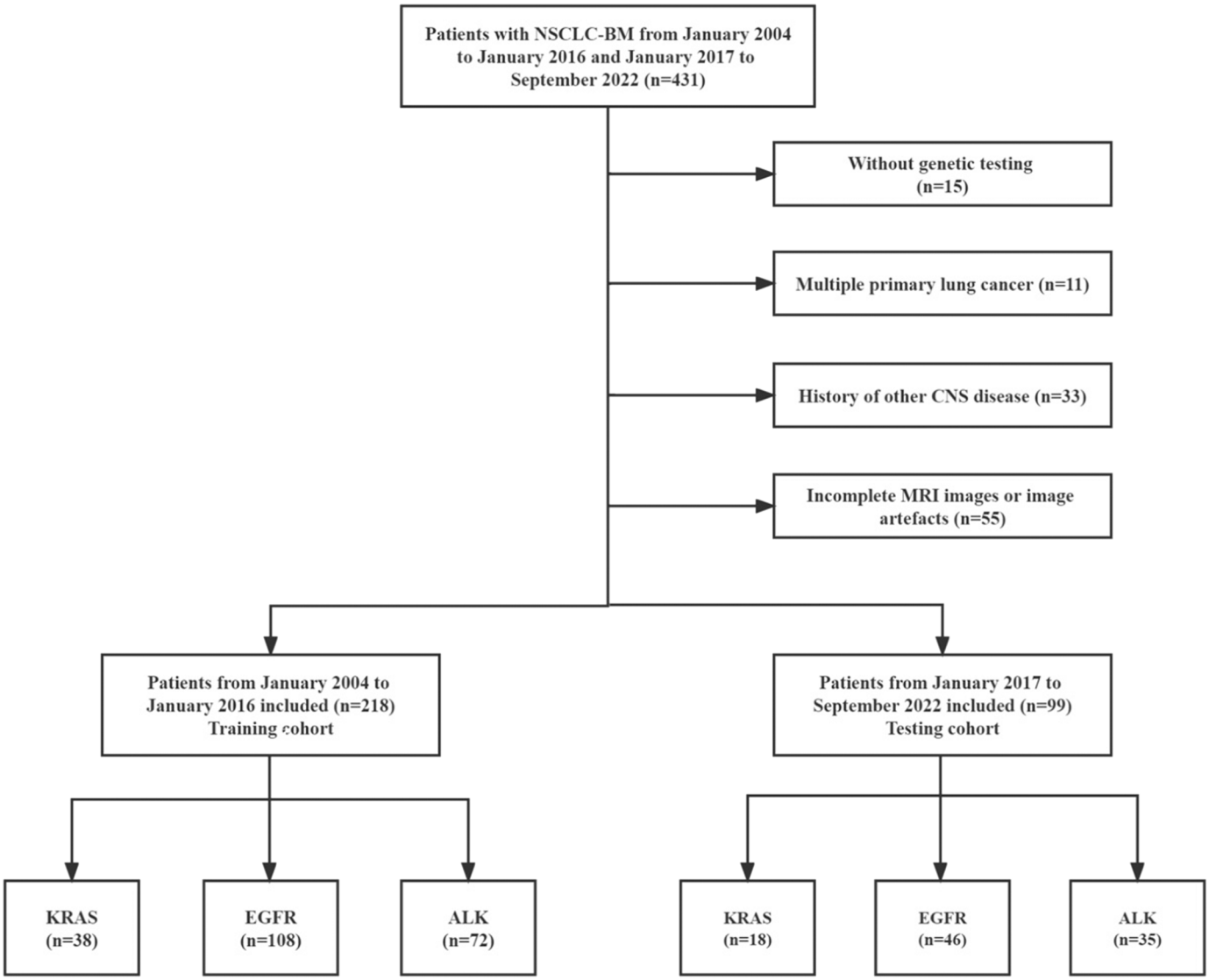

Fig. 1. The flowchart of patient selection.

The institutional ethics committee approved all the data in the study for retrospective analysis and waived the demand for informed consent.

The inclusion criteria were: (a) pathological diagnosis of NSCLC; (b) all patients had BM; (c) patients with the confirmation of KRAS, EGFR or ALK mutations in primary NSCLC or at least one of BM by surgery or biopsy; (d) all MR scans were performed before initiating treatment for BM.

The exclusion criteria were: (a) patients with multiple primary lung cancer; (b) patients with a history of other central nervous system (CNS) disease such as acute cerebral hemorrhage, infarction and so on; (c) incomplete MRI images or the existence of image artefacts.

Finally, 317 patients were enrolled in the study. Between January 2004 and January 2016, we retrospectively collected 108 patients with EGFR mutations, 72 patients with ALK rearrangements and 38 patients with KRAS mutations as the training cohort. Then an independent testing cohort which included 46 patients with EGFR mutations, 35 patients with ALK rearrangements and 18 patients with KRAS mutations was subsequently enrolled from January 2017 to September 2022. The whole patient enrollment was shown detailly in Fig. 1.

2.2. MR imaging protocol

All patients were imaged with a 3.0 T clinical MR scanner (SIGAL Pioneer, GE Healthcare, Milwaukee, Wisconsin) or 1.5 T MR scanner (Signa HDXT, GE Healthcare, Milwaukee, Wisconsin) which equipped with a sixteen channel or eight channel head coil at the time of their initial diagnosis of BM. Our MR imaging protocol for BM included routine axial T2WI (TR= 4000 ms, TE= 113 ms, slice thickness= 5 mm), axial T2 fluid-attenuated inversion recovery (T2-FLAIR) sequence (TR = 7000 ms, TE = 79 ms, inversion time (TI) = 2500 ms, slice thickness = 5 mm), axial diffusion weighted imaging (DWI) sequence with b values of 1000 s/mm^2 and 0 s/mm^2 (TR=4028 ms, TE=80 ms, slice thickness = 5 mm), and contrast-enhanced T1-weighted imaging (T1-CE) sequence (TR = 250 ms, TE = 2.46 ms, matrix = 256 × 256, FOV = 240 mm × 240 mm, slice thickness = 5 mm). Intravenous gadolinium-based contrast agent was used at a dose of 0.1 mmol/kg body weight.

2.3. BM segmentation

Registration was performed with all T2WI, T2-FLAIR, DWI and T1-CE images affinely co-registered into the same geometric space by the elastix toolbox before segmentation. Specifically, we registered T2WI, T2-FLAIR and DWI to the corresponding T1-CE sequence. Then we resampled all images to the same voxels of 3 × 3 × 3 mm^3 to balance the effect of slice thickness variation. Both these two steps were performed using 3D Slicer software (https://www.slicer.org).

The tumors segmentations were manually performed on a slice-by-slice basis using 3D slicer, an open-source 3D image analysis software. The process of segmentation was strictly contoured by an experienced radiologist and confirmed by an independent radiologist with at least 10 years of experience in brain MRI (Fig. 2). We segmented all tumors as regions of interest (ROIs) from each patient except the diameter of tumors smaller than 5 mm because they were not reliably covered in two consecutive slices, which was the minimal requirement for the 3D approach. Besides, both radiologists were blinded to the gene mutation of BM. As a result, the training cohort and testing cohort included 773 lesions and 355 lesions respectively.

2.4. Radiomics features extraction

According to ROIs, we separately extracted features based on the original images, LoG-sima-transformed images and wavlet-transformed images from four MR sequences. All of these features included seven groups: first-order features, shape-based features, grey level co-

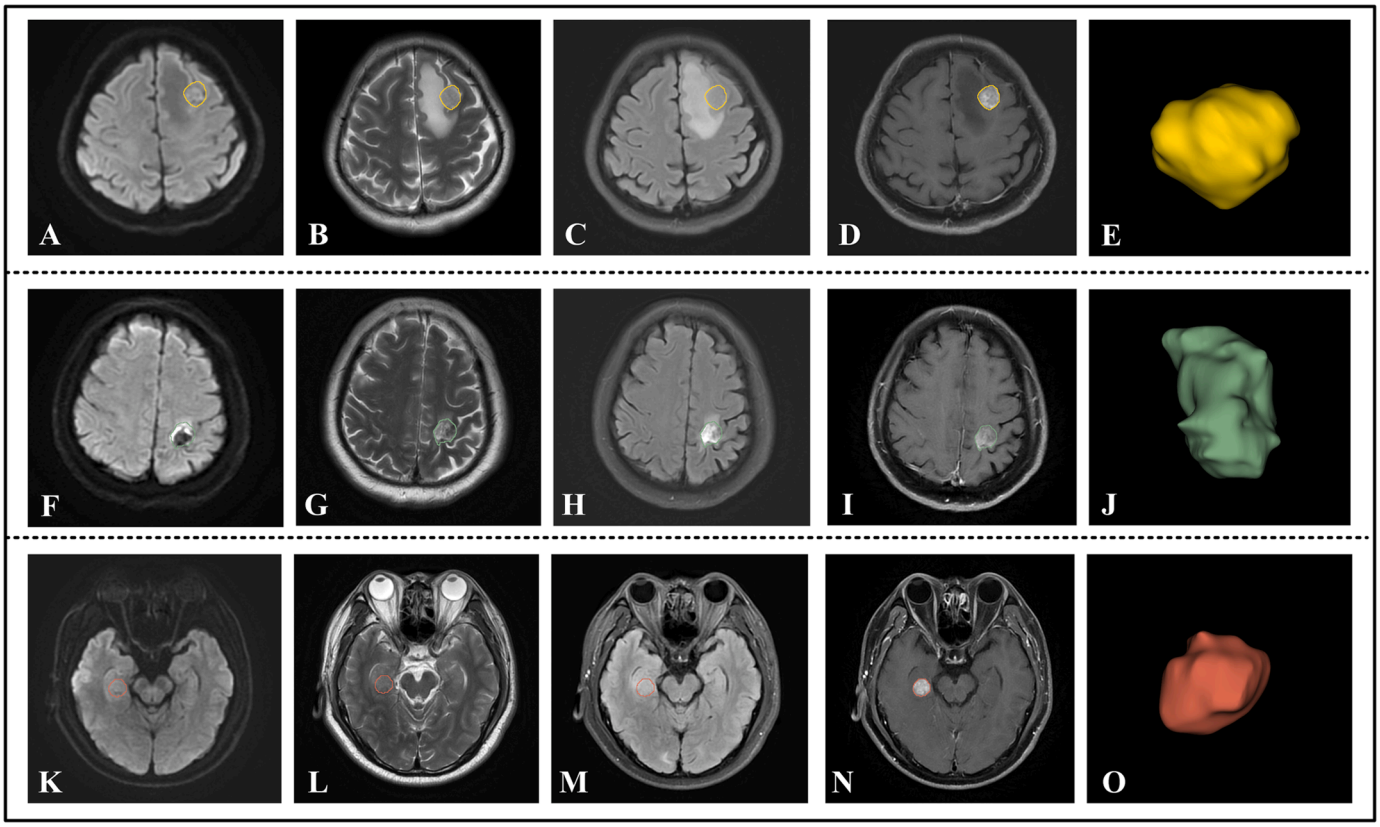

Fig. 2. Examples of MR images of BM patients used in this study: patient who is EGFR-mutant (A-E), ALK-mutant (F-J) and KRAS-mutant (K-O). (A), (F) and (K):DWI. (B), (G) and (L):T2WI. (C), (H) and (M):T2-FLAIR. (D), (I) and (N):T1-CE. (E), (J) and (O): 3D volume construction based on the ROI.

occurrence matrix (GLCM) features, grey level run length matrix (GLRLM) features, grey level size zone matrix (GLSZM) features, grey level dependence matrix (GLDM) features, and neighbouring grey tone difference matrix (NGTDM) features. The sigma values of the LoG filter were set 5.0 to 1.0 mm. Besides, the images were filtered with a low or high bandpass filter towards to x, y, and z directions. The detailed information of the radiomics features can be found in the PyRadiomics official documentation. (https://pyradiomics.readthedocs.io/en/latest/features.html).

2.5. Radiomics feature selection

To avoid bias toward majority class cases and achieve a high classification rate, we first used the synthetic minority oversampling technique (SMOTE) in the training cohort to separately balance KRAS to EGFR or ALK mutations separately in consideration of the unbalanced nature of the training dataset. Then the maximal information coefficient (MIC) was firstly used to select the top 200 relevant features based on four MR sequences according to the MIC values. Next, the recursive feature elimination (RFE) which was very popular due to its superiority in selecting features was used to choose predictable features and eliminate weak features. A tenfold cross-validation was utilized to avoid overfitting. According to the cross-validated score, we separately chose the ultimate features based on four MR sequences and visualized them.

2.6. Model construction

We used the random forest classifier (RFC) to construct the predictive models because of its high variance-bias trade-off capability. Then we built four models based on BM from each MR sequence to discriminate KRAS from EGFR mutations. Besides, models based on four MR sequences for differentiating KRAS from ALK mutations were built using RFC method. The training cohorts were randomly divided into two parts by the ratio of 7:3. Then all these models were trained and validated in the corresponding training cohort using tenfold cross validation. At last, the best model which was separately selected from all models was tested in the independent testing cohort. Feature selections and model construction were carried out by the Python scikit-learn package (version 3.8, Scikit-learn Version 0. 21, http://scikit-learn.org/).

2.7. Statistical analysis

We used the statistical analysis package in the SPSS software (version 26) and the Python Scikit-learn package. Qualitative variables were presented as frequencies and differences among groups were assessed by chi-squared tests. The continuous variable (age) was compared with t test. Receiver operator characteristic (ROC) curves and the area under the ROC curve (AUC) were used for assessing the ability of the radiomics features to predict the mutational status. Thereafter, we also evaluated accuracy, precision (positive predictive value), recall (sensitivity) and F1 score which was the harmonic average of the precision and recall, ranging from 0 to 1. For the statistical analysis, $p < 0.05$ was considered statistically significant.

3. Results

3.1. Basic clinical characteristics

The basic clinical characteristics of the 317 patients were summarized in Table 1. Our research showed that smoking has significant difference in KRAS compared to EGFR or ALK mutations whether in the training or testing cohort. As for the remaining clinical characteristics which included sex, age and alcohol consumption, there were no significant difference among three gene mutations between two cohorts.

3.2. Radiomics features selection

In models of KRAS and EGFR mutations, we selected 22 most important predictive biomarkers based on T2WI, 22 features based on DWI, 21 features based on T2-FLAIR and 18 features based on T1-CE because of the highest cross-validated score as shown in Fig. S1. As for models of discriminating KRAS and ALK mutations, 11 features based on T2WI, 23 features based on DWI, 26 features based on T2-FLAIR and 13 features based on T1-CE were respectively selected. The number of selected features for these four models were shown in Fig. S2.

3.3. Model performance

The performance of models for discriminating KRAS and EGFR mutations based on four MR sequences in both training and testing cohorts

Table 1
Clinical characteristics from KRAS, EGFR and ALK in training cohort and testing cohort.

Characteristic	Training cohort (n = 218)					Testing cohort (n = 99)				
	KRAS	EGFR	ALK	*p*	*p*	KRAS	EGFR	ALK	*p*	*p*
	(n = 38)	(n = 108)	(n = 72)	(KRAS+/EGFR+)	(KRAS+/ALK+)	(n = 18)	(n = 46)	(n = 35)	(KRAS+/EGFR+)	(KRAS+/ALK+)
Gender, n (%)										
Male	20 (52.63)	47 (43.52)	32 (44.44)	0.332	0.413	9 (50.00)	17 (36.96)	23 (65.71)	0.339	0.268
Female	18 (47.37)	61 (56.48)	40 (55.56)			9 (50.00)	29 (63.04)	12 (34.29)		
Age (mean±SD years)	61.4 ± 7.8	58.6 ± 10.1	58.9 ± 8.3	0.123	0.128	65.6 ± 8.1	62.0 ± 11.1	62.9 ± 6.4	0.216	0.190
Alcohol consumption, n (%)										
Yes	11 (28.95)	21 (19.44)	14 (19.44)	0.223	0.258	7 (38.89)	8 (17.39)	8 (22.86)	0.068	0.220
No	27 (71.05)	87 (80.56)	58 (80.56)			11 (61.11)	38 (82.61)	27 (77.14)		
Smoking, n(%)										
Yes	30 (78.95)	35 (32.41)	27 (37.50)	* < 0.001	* < 0.001	10 (55.56)	11 (23.91)	8 (22.86)	*0.015	*0.017
No	8 (21.05)	73 (67.59)	45 (62.50)			8 (44.44)	35 (76.09)	27 (77.14)		

Note: Differences were assessed by t test or chi-square test. SD: standard deviation.
* $p < 0.05$.

was shown in Fig. 3. The DWI and T2WI models yielded an AUC of 0.942 (95% CI, 0.911 to 0.967) and 0.942 (95% CI, 0.914 to 0.967), F1 score of 0.890 and 0.877, which were confirmed in the testing cohort with an AUC of 0.949 (95% CI, 0.899 to 0.986) and 0.954 (95% CI, 0.905 to 0.993), F1 score of 0.903 and 0.933. The T1-CE model yielded an AUC of 0.918 (95% CI, 0.882 to 0.949) and 0.954 (95% CI, 0.890 to 0.996) and F1 score of 0.826 and 0.900. The AUCs and F1 scores of T2-FLAIR model were 0.956 (95% CI, 0.929 to 0.978) and 0.838 (95% CI, 0.750 to 0.918) and 0.903 and 0.733 in two cohorts. Table 2 summarizes the accuracy, precision, recall and F1 score of these four models in two cohorts.

As for models of differentiating KRAS from ALK mutations, the AUCs of the DWI model are 0.947 (95% CI, 0.915 to 0.974) and 0.850 (95% CI, 0.735 to 0.944) in the training and testing cohort. And the F1 scores of the DWI model are 0.871 and 0.750 in the two cohorts respectively. The T2-FLAIR model achieved an AUC of 0.917 (95% CI, 0.875 to 0.952) and 0.824 (95% CI, 0.705 to 0.924), F1 score of 0.837 and 0.708. The AUCs and F1 scores of the T2WI and T1-CE model were 0.896 (95% CI, 0.849 to 0.940) and 0.892 (95% CI, 0.847 to 0.933), 0.831 and 0.824 in the training cohort, 0.795 (95% CI, 0.664 to 0.912) and 0.790 (95% CI, 0.668 to 0.902), 0.739 and 0.766 in the testing cohort. The ROC curves and AUCs of these models in the training and testing cohorts are shown in Fig. 4. Besides, Table 3 summarizes the accuracy, precision, recall and F1 score of these three models in two cohorts.

4. Discussion

In this study, we proposed a retrospective radiomics analysis and developed non-invasive quantitative biomarkers using machine learning algorithms based on four normalized MR sequences (T1-CE, T2-FLAIR, T2WI and DWI) of BM to differentiate KRAS from EGFR or ALK mutations. Finally, we found that radiomics models of multisequence MRI have the potential to differentiate mutation status in BM.

This study collected basic clinical characteristics of all patients. The analysis showed that the smoking history of KRAS mutations patients had statistical significance with EGFR or ALK mutations patients in two cohorts. It was consistent with previous studies that KRAS mutations was associated with smokers whereas EGFR or ALK mutations was commonly observed in never or lighter smokers [15]. In terms of other characteristics such as sex, age and alcohol consumption, there was no significant difference among three mutations in two cohorts.

Numerous previous studies have reported the capacity of CT image-based radiomics to predict genetic status in LC [21–23]. Tu et al. [21] compared the performance of radiomics signature and CT morphological features for predicting EGFR mutation status, and showed that the radiomics features perform better with an AUC of 0.762 in the training cohort. Cheng et al. [22] established a radiomics model with 102 selected features and presented an encouraging discrimination performance to identify mutant and wild-type EGFR in ground-glass opacity featured lung adenocarcinoma with an AUC of 0.846 and 0.816 for the training and testing cohorts respectively. However, compared with these radiomics analysis based on the images of primary lung tumors, we mainly concentrated on features extracted from BM lesions.

There are several reasons for us to choose MR-based radiomics to identify KRAS mutations. Firstly, brain was the most frequent metastatic site for NSCLC and initial site of relapse after treatment [11]. Recent clinical practice guidelines have recommended that it is mandatory for all locally advanced and metastatic NSCLC patients to perform molecular testing including EGFR, ALK and KRAS [24]. Whereas, biopsy is invasive and polygenic testing is expensive. Currently, MRI has evolved to become the standard method to diagnose and monitor BM with excellent soft tissue contrast [25]. Secondly, nearly 80% patients discovered BM after primary tumor already has been diagnosed which means metachronous diagnosis [26]. Thus, it was always infeasible to extract radiomics features from primary lesions of these patients who have underwent a wide range of treatments such as radiotherapy, chemotherapy and even surgical resection. Finally, with the development of MRI, increasing number of small BM in asymptomatic patients can be detected even prior to the primary LC [27]. As a result, our models based on BM radiomics signature could be served as a proper complementary and alternative method to predict mutation status that is desirable than relying solely on primary lesions. Previously, we have already indicated that radiomics features based on regular MR sequences have significant values in distinguishing EGFR mutations from ALK rearrangements in BM [27]. Wang et al. [28] developed MR-based radiomics signature of BM to predict EGFR mutations and found that the T2-FLAIR model achieved the best performance. Chen and colleagues [8] demonstrated that radiomics analysis of BM could be used to classify genetic mutations. In their study, the combined models of radiomics features and clinical characteristics yielded AUC values of 0.912, 0.915 and 0.985 for classification of EGFR, ALK and KRAS mutation status respectively. The predictive ability of the models in above reports is satisfactory which demonstrated that radiomics based on BM can reflect

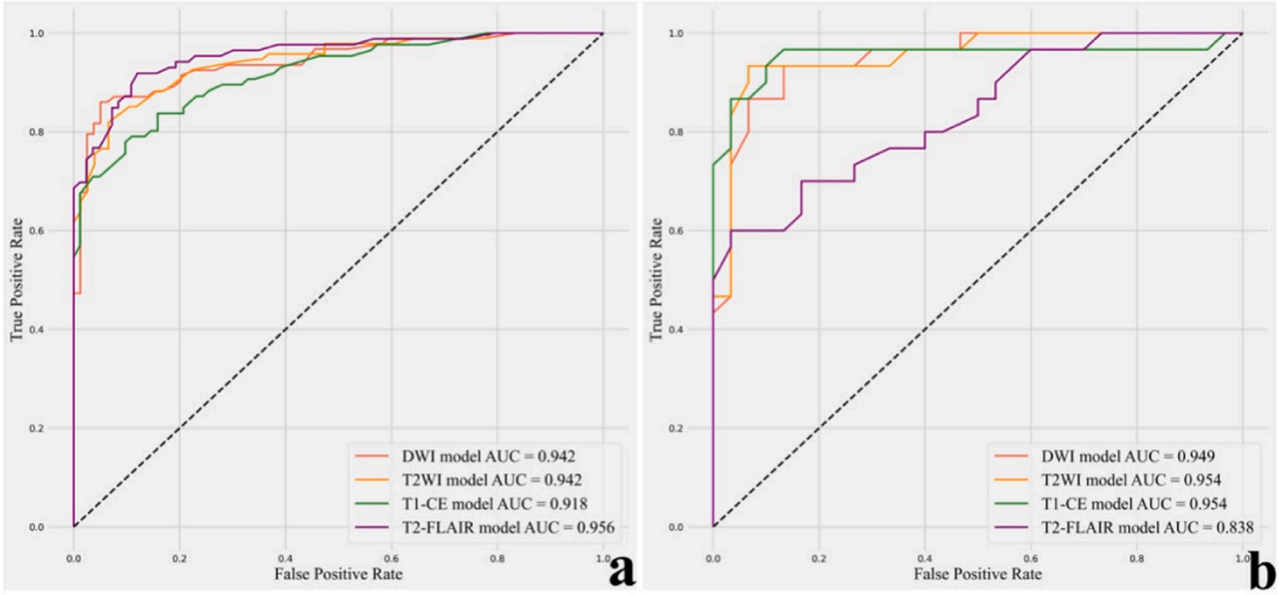

Fig. 3. ROC curves of models for discriminating KRAS from EGFR mutations. (a) Training cohort. (b) Testing cohort.

Table 2
Predictive performance of four models in discriminating KRAS and EGFR.

Index	Training cohort				Testing cohort			
	DWI model	T2WI model	T2-FLAIR model	T1-CE model	DWI model	T2WI model	T2-FLAIR model	T1-CE model
AUC	0.942	0.942	0.956	0.918	0.949	0.954	0.838	0.954
Accuracy	0.884	0.865	0.899	0.827	0.900	0.933	0.733	0.900
Precision	0.910	0.882	0.888	0.852	0.875	0.933	0.733	0.900
Recall	0.871	0.872	0.919	0.802	0.933	0.933	0.733	0.900
F1 score	0.890	0.877	0.903	0.826	0.903	0.933	0.733	0.900

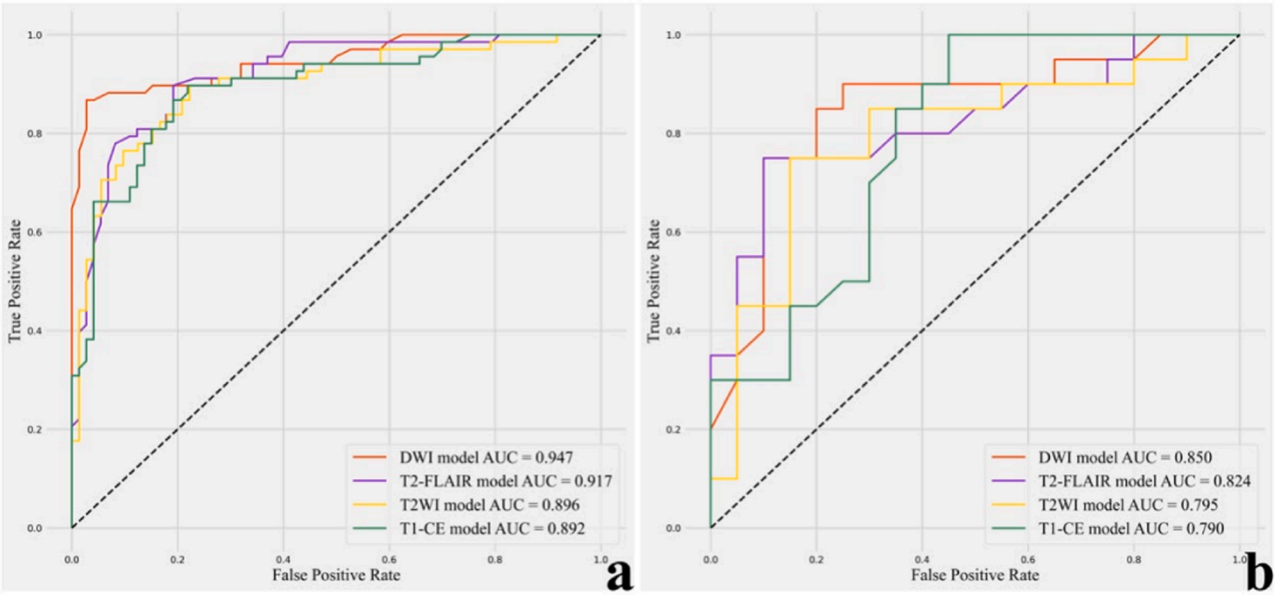

Fig. 4. ROC curves of models for discriminating KRAS from ALK mutations. (a) Training cohort. (b) Testing cohort.

Table 3
Predictive performance of four models in discriminating KRAS and ALK.

Index	Training cohort				Testing cohort			
	DWI model	T2WI model	T2-FLAIR model	T1-CE model	DWI model	T2WI model	T2-FLAIR model	T1-CE model
AUC	0.947	0.896	0.917	0.892	0.850	0.795	0.824	0.790
Accuracy	0.871	0.829	0.837	0.816	0.700	0.700	0.650	0.725
Precision	0.847	0.797	0.808	0.763	0.643	0.654	0.607	0.667
Recall	0.897	0.868	0.868	0.897	0.900	0.850	0.850	0.900
F1 score	0.871	0.831	0.837	0.824	0.750	0.739	0.708	0.766

mutation status effectively.

Current researches of radiomics signature based on MR images of BM have paid extensive attention on detecting EGFR and ALK mutations but limited attention to KRAS mutations. Nevertheless, KRAS mutations is estimated to comprise a quarter of NSCLC and typically mutually exclusive with other clinically actionable mutation types including EGFR and ALK [15,29]. Pao et al. [30] have indicated that mutations in KRAS is associated with primary resistance to erlotinib and gefitinib which are both EGFR Tyrosine kinase inhibitors. Thus, distinguishing KRAS mutations from the two common mutation status (EGFR or ALK) in NSCLC can guide the selection of these kinase inhibitors. Targeting KRAS has long been marked by frustration due to the lack of unknown drug-pockets and anti-EGFR treatment [31,32]. Recently, KRAS has evolved from a genotype with predictive value to a therapeutic target recently with the observation of sotorasib——an inhibitor of the KRAS G12C approved by the FDA [31,33]. The numbers of clinical trials are ongoing to explore the mechanism of resistance pathways and novel agents targeting KRAS [34,35]. Therefore, early identifying KRAS mutations and appealing these patients to participate in clinical investigations can not only evaluate novel agents and strategies but also bring patients with KRAS-mutant LC hope for long-sought goal of cure.

In our current study, both two DWI models showed excellent performance in discriminating KRAS from EGFR or ALK mutations with AUCs of 0.942, 0.947 in the training cohort and 0.949, 0.850 in the testing cohort respectively. Previous studies have demonstrated that the DWI sequence has a moderate diagnostic value for differentiating primary brain tumors from solitary BM and identifying the histology of BM from NSCLC [17,18]. The results of Jung et al. suggested that DWI parameters can also predict EGFR mutation status in BM [19]. These findings have indicated that DWI can reflect potential molecular and genetic information well through detecting motion of water altered by disease. Besides, the radiomics models for T2WI sequence can differentiate KRAS from EGFR with high AUCs in two cohorts while the models for T2-FLAIR sequence can identify KRAS and ALK accurately. F1-score relies on the associated precision and recall, as the score varies more when the dataset is imbalanced, which is commonly used when developing prediction models in medicine [20]. Among the KRAS+ /EGFR+ classification models in our research, the T2-FLAIR

model yielded the F1-score of 0.903 in the training cohort but 0.733 in the testing cohort, whereas the F1-scores of the other three models were relatively high particularly in the testing cohort all up to 0.90, which may indicate that the radiomics models for discriminating KRAS+ /EGFR+ in our study have better predictive performance when the datasets are imbalanced. However, the F1-scores of the four KRAS+ /ALK+ classification models ranged from 0.824 to 0.871 in the training set and 0.708 to 0.766 in the testing set were moderate. In addition, we found that all metrics of KRAS+ /EGFR+ classification models performed better than those of KRAS+ /ALK+ models, which may be related to the smaller dataset of ALK-mutant patients compared to EGFR mutations.

There were several limitations of our study. Firstly, it was a retrospective single-institutional study and more prospective multicentric studies should be carried out to reduce the deviation of regional characteristics. However, we recruited BM patients from two time points which may reduce the impact partly. Secondly, with a total of 317 patients, the sample size of our study is still modest although it is larger than similar studies.

In summary, our study has demonstrated that radiomics classifiers integrating multisequence MRI may have potential to identify KRAS mutations, especially DWI and T2WI radiomics model when compared to EGFR mutations, DWI and T2-FLAIR radiomics model when compared to ALK mutations. They are helpful to guide clinical therapeutic strategies and facilitate the discovery of new approaches capable of achieving this long-sought goal of cure in populations of patients with KRAS-mutant NSCLC.

Funding

This work was supported by Leading Talents of Beijing Tongzhou District High Level Talent Development Support Project [YHLD2019029]; and Talent Development Plan for High-level Public Health Technical Personnel Project [G2024-2-004].

Ethical statement

The ethics review board of Beijing Chest Hospital, Capital Medical University hospital approved this retrospective analysis and waived the need for written informed consent.

CRediT authorship contribution statement

Wang Bing: Visualization, Methodology, Investigation, Formal analysis, Data curation. **Li Ye:** Writing – review & editing, Writing – original draft, Visualization, Validation, Supervision, Software, Methodology, Conceptualization. **Lv Xinna:** Writing – review & editing, Writing – original draft, Supervision, Software, Methodology, Formal analysis, Data curation, Conceptualization. **Hou Dailun:** Writing – review & editing, Supervision, Resources, Project administration, Methodology, Funding acquisition, Conceptualization. **Xu Zexuan:** Writing – review & editing, Visualization, Validation, Data curation. **Wang Yichuan:** Writing – original draft, Visualization, Validation, Formal analysis, Data curation.

Declaration of Competing Interest

The authors declare that they have no known competing financial interests or personal relationships that could have appeared to influence the work reported in this paper.

Acknowledgements

This research was supported by Leading Talents of Beijing Tongzhou District High Level Talent Development Support Project [YHLD2019029]; and Talent Development Plan for High-level Public Health Technical Personnel Project [G2024–2-004]. The funding source provided financial support without any influence on the study design and interpretation of data.

Appendix A. Supporting information

Supplementary data associated with this article can be found in the online version at doi:10.1016/j.ejro.2024.100548.

References

[1] C. Nolan, L.M. Deangelis, Overview of metastatic disease of the central nervous system, Handb. Clin. Neurol. 149 (2018) 3–23.
[2] X. Jiang, M. Ren, X. Shuang, et al., Multiparametric MRI-based radiomics approaches for preoperative prediction of EGFR mutation status in spinal bone metastases in patients with lung adenocarcinoma, J. Magn. Reson Imaging 54 (2) (2021) 497–507.
[3] R.S.P. Huang, L. Harries, B. Decker, et al., Clinicopathologic and genomic landscape of non-small cell lung cancer brain metastases, Oncologist 27 (10) (2022) 839–848.
[4] R.C. Doebele, X. Lu, C. Sumey, et al., Oncogene status predicts patterns of metastatic spread in treatment-naive nonsmall cell lung cancer, Cancer 118 (18) (2012) 4502–4511.
[5] K.L. Johung, N. Yeh, N.B. Desai, et al., Extended survival and prognostic factors for patients with alk-rearranged non-small-cell lung cancer and brain metastasis, J. Clin. Oncol. 34 (2) (2016) 123–129.
[6] D.Y. Shin, I.I. Na, C.H. Kim, S. Park, H. Baek, S.H. Yang, Egfr mutation and brain metastasis in pulmonary adenocarcinomas, J. Thorac. Oncol. 9 (2014) 195–199.
[7] A. Friedlaender, A. Drilon, G.J. Weiss, G.L. Banna, A. Addeo, KRAS as a druggable target in NSCLC: Rising like a phoenix after decades of development failures, Cancer Treat. Rev. 85 (2020) 101978.
[8] B.T. Chen, T. Jin, N. Ye, et al., Radiomic prediction of mutation status based on MR imaging of lung cancer brain metastases, Magn. Reson Imaging 69 (2020) 49–56.
[9] S.R. Punekar, V. Velcheti, B.G. Neel, K.K. Wong, The current state of the art and future trends in RAS-targeted cancer therapies, Nat. Rev. Clin. Oncol. 19 (10) (2022) 637–655.
[10] E. Rios Velazquez, C. Parmar, Y. Liu, J. Quackenbush, H.J.W.L. Aerts, et al., Somatic mutations drive distinct imaging phenotypes in lung cancer, Cancer Res 77 (14) (2017) 3922–3930.
[11] X. Lin, L.M. DeAngelis, Treatment of brain metastases, J. Clin. Oncol. 33 (30) (2015) 3475–3484.
[12] M.E. Mayerhoefer, A. Materka, G. Langs, et al., Introduction to radiomics, J. Nucl. Med 61 (4) (2020) 488–495.
[13] T. Zhang, Z. Xu, G. Liu, et al., Simultaneous identification of EGFR,KRAS,ERBB2, and TP53 mutations in patients with non-small cell lung cancer by machine learning-derived three-dimensional radiomics, Cancers (Basel) 13 (8) (2021) 1814.
[14] W. Tu, G. Sun, L. Fan, et al., Radiomics signature: a potential and incremental predictor for EGFR mutation status in NSCLC patients, comparison with CT morphology, Lung Cancer 132 (2019) 28–35.
[15] R.A. de Mello, P. Madureira, L.S. Carvalho, A. Araújo, M. O'Brien, S. Popat, EGFR and KRAS mutations, and ALK fusions: current developments and personalized therapies for patients with advanced non-small-cell lung cancer, Pharmacogenomics 14 (14) (2013) 1765–1777.
[16] Y. Li, X. Lv, B. Wang, et al., Predicting EGFR T790M mutation in brain metastases using multisequence mri-based radiomics signature, Acad. Radiol. S1076-6332 (22) (2022) 00686–00689.
[17] P. Zhang, B. Liu, Differentiation among glioblastomas, primary cerebral lymphomas, and solitary brain metastases using diffusion-weighted imaging and diffusion tensor imaging: a PRISMA-compliant meta-analysis, ACS Chem. Neurosci. 11 (3) (2020) 477–483.
[18] G. Duygulu, G.Y. Ovali, C. Calli, et al., Intracerebral metastasis showing restricted diffusion: correlation with histopathologic findings, Eur. J. Radio. 74 (2010) 117–120.
[19] W.S. Jung, C.H. Park, C.K. Hong, S.H. Suh, S.J. Ahn, Diffusion-weighted imaging of brain metastasis from lung cancer: correlation of MRI parameters with the histologic type and gene mutation status, AJNR Am. J. Neuroradiol. 39 (2) (2018) 273–279.
[20] Z. DeVries, E. Locke, M. Hoda, et al., Using a national surgical database to predict complications following posterior lumbar surgery and comparing the area under the curve and F1-score for the assessment of prognostic capability, Spine J. 21 (7) (2021) 1135–1142.
[21] W. Tu, G. Sun, L. Fan, et al., Radiomics signature: a potential and incremental predictor for EGFR mutation status in NSCLC patients, comparison with CT morphology, Lung Cancer 132 (2019) 28–35.
[22] B. Cheng, H. Deng, Y. Zhao, et al., Predicting EGFR mutation status in lung adenocarcinoma presenting as ground-glass opacity: utilizing radiomics model in clinical translation, Eur. Radio. 32 (9) (2022) 5869–5879.
[23] T.Y. Jia, J.F. Xiong, X.Y. Li, et al., Identifying EGFR mutations in lung adenocarcinoma by noninvasive imaging using radiomics features and random forest modeling, Eur. Radio. 29 (9) (2019) 4742–4750.
[24] E.N. Imyanitov, A.G. Iyevleva, E.V. Levchenko, Molecular testing and targeted therapy for non-small cell lung cancer: Current status and perspectives, Crit. Rev. Oncol. Hematol. 157 (2021) 103194.

[25] K.J. Langen, N. Galldiks, E. Hattingen, N.J. Shah, Advances in neuro-oncology imaging, Nat. Rev. Neurol. 13 (5) (2017) 279–289.
[26] P. Sacks, M. Rahman, Epidemiology of brain metastases, Neurosurg. Clin. N. Am. 31 (4) (2020) 481–488.
[27] Y. Li, X. Lv, B. Wang, Z. Xu, Y. Wang, Differentiating EGFR from ALK mutation status using radiomics signature based on MR sequences of brain metastasis, Eur. J. Radio. 155 (2022) 110499.
[28] L. Zheng, H. Xie, X. Luo, et al., Radiomic signatures for predicting EGFR mutation status in lung cancer brain metastases, Front Oncol. 12 (2022) 931812.
[29] J.D. Campbell, A. Alexandrov, J. Kim, J. Wala, et al., Distinct patterns of somatic genome alterations in lung adenocarcinomas and squamous cell carcinomas, Nat. Genet. 48 (2016) 607–616.
[30] W. Pao, T.Y. Wang, G.J. Riely, et al., KRAS mutations and primary resistance of lung adenocarcinomas to gefitinib or erlotinib, PLoS Med 2 (1) (2005) e17.
[31] A. Feng, Y. Li, G. Li, et al., Genomic features of organ-specific metastases in lung adenocarcinoma, Front Oncol. 12 (2022) 908759.
[32] D. Zhao, H. Li, I. Mambetsariev, T. Mirzapoiazova, et al., Clinical and molecular features of KRAS-mutated lung cancer patients treated with immune checkpoint inhibitors, Cancers 14 (19) (2022) 4933.
[33] F. Skoulidis, B.T. Li, G.K. Dy, et al., Sotorasib for lung cancers with KRAS p.G12C mutation, N. Engl. J. Med 384 (25) (2021) 2371–2381.
[34] D.S. Hong, M.G. Fakih, J.H. Strickler, et al., $KRAS^{G12C}$ inhibition with sotorasib in advanced solid tumors, N. Engl. J. Med 383 (13) (2020) 1207–1217.
[35] F. McCormick, Progress in targeting RAS with small molecule drugs, Biochem J. 476 (2) (2019) 365–374.